HHS Public Access

Author manuscript

J Magn Reson Imaging. Author manuscript; available in PMC 2016 March 09.

Published in final edited form as:

J Magn Reson Imaging. 2014 October ; 40(4): 875–883. doi:10.1002/jmri.24457.

T1 Bias in Chemical Shift-Encoded Liver Fat-Fraction: Role of the Flip Angle

Jens-Peter Kuhn, MD[1,*], **Christina Jahn**[1], **Diego Hernando, PhD**[2], **Werner Siegmund, MD**[3], **Stefan Hadlich**[1], **Julia Mayerle, MD**[4], **Jorg Pfannmoller, PhD**[1], **Sonke Langner, MD**[1], and **Scott Reeder, MD**[2,5]

[1]Department of Radiology and Neuroradiology, University Greifswald, Greifswald, Germany

[2]Department of Radiology, University of Wisconsin, Madison, Wisconsin, USA

[3]Department of Clinical Pharmacology, University Greifswald, Greifswald, Germany

[4]Department of Medicine, University Greifswald, Greifswald, Germany

[5]Departments of Medical Physics, Biomedical Engineering and Medicine, University of Wisconsin, Madison, Wisconsin, USA

Abstract

Purpose—To investigate flip angle (FA)-dependent T1 bias in chemical shift-encoded fat-fraction (FF) and to evaluate a strategy for correcting this bias to achieve accurate MRI-based estimates of liver fat with optimized signal-to-noise ratio (SNR).

Materials and Methods—Thirty-three obese patients, 14 men/19 women, aged 57.3 ±13.9 years underwent 3 Tesla (T) liver MRI including MR-spectroscopy and four three-echo-complex chemical shift-encoded MRI sequences using different FAs (1°/3°/10°/20°). FF was estimated with R2* correction and multi-peak fat spectral modeling. The FF for each FA with and without T1 correction was compared with spectroscopy as a reference standard, using linear regression. Relative SNR of the magnitude data were assessed for each flip angle.

Results—The correlation between chemical shift-encoded MRI and spectroscopy was high ($R^2 \asymp 0.9$). Without T1 correction, the agreement of both techniques showed no significant differences in slope ($P_{FlipAngle1^\circ} = 0.385/P_{FlipAngle3^\circ} = 0.289$) using low FA. High FA resulted in significant different slopes ($P_{FlipAngle10^\circ} = 0.016/P_{FlipAngle20^\circ} = 0.014$. T1 bias was successfully corrected using the T1 correction strategy (slope:$P_{FlipAngle10^\circ} = 0.387/P_{FlipAngle20^\circ} = 0.440$). Additionally, the use of high FA (near the Ernst angle) improved the SNR of the magnitude data (*FA1 vs. FA3; respectively FA1 vs. FA10* $P \leq 0.001$).

Conclusion—T1 bias is a strong confounder in the assessment of liver fat using chemical shift imaging with high FA. However, using a larger flip angle with T1 correction leads to higher SNR, and residual error after T1 correction is very small.

[*]Address reprint requests to: J.-P.K., Department of Radiology and Neuroradiology, Ernst Moritz Arndt University Greifswald, Ferdinand-Sauerbruch-Straße NK, Greifswald, D-17475; Germany. kuehn@uni-greifswald.de.

Keywords

liver; fatty liver; magnetic resonance imaging; chemical shift imaging; magnetic resonance spectroscopy

MRI is a promising tool for the assessment of fat in tissue (1,2). MR-based techniques for routine clinical detection and quantification of tissue fat are well established for the liver and are of great interest in other organs and tissue such as the pancreas, bone marrow, and muscle (3–6). One simple approach for tissue fat detection is the technique of in-phase/out-of-phase chemical shift imaging (7,8). The chemical shift technique is based on differences in the resonance frequencies of protons of water and triglycerides. Recent studies have shown the chemical shift in-phase/out-of-phase approach to be suitable for clinical liver fat detection and a promising candidate for liver fat quantification (9,10).

However, in-phase/out-of-phase imaging is limited by the effects of confounding factors (11), such as T2* bias, T1 bias, and the multi-peak spectral complexity of fat (12–15). Several recent techniques have been developed that acquire multiple gradient echo images acquired at increasing echo times and perform fat quantification by correcting for all relevant confounders. If all confounders are considered, the calculated fat-fraction (FF) becomes the proton-density-fat fraction (PDFF) (16). Confounder-corrected mapping of PDFF allows reliable quantification of tissue fat, with robustness to varying scan parameters (14,15) and reproducibility across MR scanners (17). Emerging quantitative techniques include confounder-corrected magnitude chemical shift-encoded MRI, restricted to FF below 50%, and confounder-corrected complex chemical shift-encoded MRI, for quantifying FF from 0–100% (1,18).

T1 bias is a strong confounder for MR-based fat quantification. Fat and water have different T1 relaxation times, and this difference introduces errors in tissue fat quantification if the underlying acquisition is T1-weighted (19). For gradient-echo acquisitions, there are two strategies to generate T1-independent FF - the use of long repetition times (TR) and the use of low flip angles (20). Unfortunately, long TR values lengthen the acquisition and result in infeasible breath-hold acquisition times, particularly for three-dimensional (3D) gradient-echo imaging. The use of low flip angles to reduce T1 bias in liver imaging has been proposed by several authors (16,19,21). Specifically, for 3D techniques, flip angles of 5° for 1.5 Tesla (T) (15) and 3° for 3T (14) have been described and shown to effectively avoid T1 bias in fat quantification. However, the use of small flip angles leads to low signal-to-noise ratios (SNRs) of the underlying data.

Several recent works have investigated this tradeoff between T1 bias and SNR in chemical shift-encoded fat quantification. Hines et al introduced a mathematical framework to design SNR-optimized chemical shift-encoded fat quantification acquisitions, given a maximum allowed T1 bias (20). Johnson et al investigated the T1 bias for liver fat quantification using combinations of different TRs (7/14 ms) and relatively low flip angles (1–5° for 3D imaging) (22). The errors due to T1 effects increased as a function of the flip angle. However, the use of high image flip angles increases the signal-to-noise (SNR). At this time, it is not clear whether this higher SNR is advantageous for liver fat quantification.

An alternative approach for fat quantification free of T1 bias is to perform acquisitions with high flip angles (closer to the Ernst angle), and correct for T1 bias by postprocessing, using either measured (23) or assumed T1 values for water and fat. This approach has been used successfully in the lumbar spine (23). The impact of SNR-optimized MRI on the noise performance of liver fat quantification (PDFF) and liver iron quantification (R2* mapping) is unknown.

Therefore, the purpose of our study was to identify the optimal image flip angle for liver fat quantification while avoiding errors caused by T1 bias and errors resulting from low SNR. Furthermore, a simple reconstruction technique (20) was used to correct for T1 errors and to calculate an SNR-optimized T1-independent FF. A second purpose of this study was to determine whether the SNR of the underlying image data influences the estimation of R2*.

MATERIAL AND METHODS

This prospective study was approved by the local ethics committee of the University hospital in Greifswald, Germany. Patients were included in the setting of GANI-Med (Greifswald Approach to Individualized Medicine) and the Optifast project. Both projects include an MRI examination for assessing liver fat. All patients were informed and consented to the MRI examination and inclusion in the study.

Study Population

Between November 2012 and June 2013, a total of 35 patients underwent prospective liver MRI to assess liver fat content. The exam included MR spectroscopy (MRS) and several chemical shift-encoded imaging acquisitions. Subjects included 20 women and 15 men with a mean age of 57.3 ± 13.5 years. Inclusion criteria were (1) sonographically detected liver steatosis and/or (2) a body mass index (BMI) above 25 kg/m^2. Subjects with contraindications to MRI, such as pacemakers, MR-incompatible metal implants, and claustrophobia, were excluded. In additional, two subjects were excluded from analysis because of incorrect placement of the MRS voxel. In these subjects, MRS and the general FF quantified using chemical shift MRI were fundamentally different (25.8% and 33.9% using MRS versus 2.6% and 2.2% using chemical shift MRI).

The final comparison of MRS and chemical shift-encoded MRI included 33 patients, 19 women and 14 men, with a mean age of 57.3 ± 13.9 years.

MR Imaging and Spectroscopy

MRI was performed using a commercially available 3 Tesla clinical MRI system (Verio; Siemens Healthcare, Erlangen, Germany). Images were acquired with patients in supine position using a combination of the spine array (two channels) and the body array receiver coil (four channels).

The imaging protocol included a multi-echo chemical shift-encoded gradient-echo (GRE) sequence and acquisitions with different flip angles of 1°, 3°, 10°, and 20°. Image parameters for the three-echo chemical shift-encoded technique included: repetition time (TR) = 6.51 ms; echo time $(TE)_{1/2/3}$ = 1.22/2.45/4.90 ms; number of averages = 1; echo train

length = 3; bandwidth = ± 914 Hz/pixel; imaging matrix = 288 × 125; field of view (FOV) = 450 × 300 mm; parallel acquisition (GRAPPA) with an acceleration factor of 2 and 24 reference lines, slice partial Fourier factor of 0.75; slice thickness = 6.0 mm; 32 slices. Spatial resolution was 1.6 × 2.4 × 6 mm^3 interpolated to 0.8 × 0.8 × 3.0 mm^3. Each flip angle was acquired in a separate 9-s breath-hold. Patients were instructed to perform breath holding in the same period of inspiration to co-localize each acquisition at different flip angles as best as possible.

Finally, a T2-corrected single-voxel multi-echo ^{1}H MRS (HISTO) was acquired in a voxel placed in Couinaud segment 7 of the liver, avoiding liver lesions, large vessels and bile ducts, with the following parameters: TR = 3000 ms; $TE_{1/2/3/4/5}$: 12, 24, 36, 48, 72 ms; flip angle = 90°; bandwidth = ± 1200 Hz/pixel; voxel size 30 × 30 × 30 mm, for total acquisition time of 15s. MRS was based on a single voxel method (STEAM: Stimulated Echo Acquisition Mode). T1 bias was avoided because of the high TR used for data acquisition. The spectral complexity of fat was considered, and T2 correction was performed based on the multiple-TE acquisition using an automated on-line algorithm (24). PDFF measurements from HISTO were used as reference standard in this study.

Reconstruction

The chemical shift-encoded MRI datasets were postprocessed after acquisition to generate FF maps using a custom routine under the Matlab software package (version 7.7.0; R2008b, MathWorks, Natick, MA). The postprocessed FF values were estimated with correction for R2* and consideration of the multipeak spectral complexity of fat (25). Furthermore, correction for noise related bias was performed (19). Optionally, an additional correction of T1 recovery bias was included using a postprocessing procedure based on published T1 times at 3 Tesla for fat (382 ms) and liver water (809 ms) signal components (26). This procedure consists of removing the T1 weighting from the estimated water and fat signal amplitudes before FF calculation. This is performed by dividing these water and fat amplitudes by the gradient echo sequence contrast equation $\frac{C_{w,f}=(1-e^{-\frac{TR}{T1}}w,f)\sin(FA)}{1-e^{-\frac{TR}{T1}}w,f\cos(FA)}$ (19), using the imaging TR and the assumed T1 values for water and fat, respectively. The postprocessing method for T1-correction has been published previously (20).

FF maps were computed for each of the four flip angles used (1, 3, 10, 20°) without and with correction for T1 recovery bias. Additionally, R2* maps were generated from all magnitude images for each flip angle.

Data Analysis

Images were analyzed by one reader (C.J.) with 1 year of experience in liver MR imaging using Osirix (version 5.02, Bernex, Switzerland). The reader was aware of the liver segment where the MRS was acquired.

A region-of-interest (ROI) was placed in the in-phase magnitude images (TE_1 = 1.22 ms) avoiding areas of motion artifacts, large vessels and bile ducts, and focal liver lesions. The ROI size was at least 10 cm^2. The ROI was placed in the same liver segment where the MRS

is located. The ROI was transferred to the out-of-phase magnitude images (TE_2 = 2.45 ms) using the copy and paste function to ensure perfect colocalization. The signal intensity of the magnitude data (SI) was assessed. Additionally, the image noise (SD_{noise}) was assessed for each flip angle acquisition. For this purpose, ROIs were placed in the magnitude images (TE_1;TE_2) outside the body. Signal-to-noise ratio (SNR) for in-phase and out-of-phase images was calculated as follows:

$$\text{Absolute SNR (flipangle)} = \frac{\text{SI (eg. TE1/TE2)}}{\text{SD noise}}$$

The absolute SNR contains errors because noise will be spatially heterogeneous due to the use of parallel imaging (27–29). Because of the unknown factors, the relative SNR was calculated as follows:

$$\text{Relative SNR (flip angle x)} = \frac{\text{SNR (flip angle x)}}{\text{SNR (flip angle 1°)}}$$

The SNR of the flip angle 1, also defined as lowest SNR was defined as reference for comparisons to SNR of flip angle *x*, eg, 3°;10°;20°.

Furthermore, ROIs were copied into FF maps generated with and without T1 correction and also into the R2* maps that are automatically estimated as part of the T2*-corrected fat estimation (30). The procedure was performed separately for each flip angle. Possible misregistration between images acquired at different flip angles due to differences in breath-holding was ignored. The FF and R2* values for each image flip angle were subsequently recorded (Microsoft Excel; v.14.2.3; 2011; Microsoft Corporation, Redmond, WA).

Statistics

All quantitative values (eg, demographic data, FF estimated by MRS and chemical shift encoded imaging, and R2*) are presented as mean and standard deviation. MR spectroscopy served as the standard of reference for liver fat content.

First, the FF values measured for each flip angle, with and without correction for T1 bias, were compared with the results of MRS using linear regression analysis to evaluate the effects of flip angle and T1 correction. Perfect agreement was defined as a regression line with a slope of 1 and an intercept of 0%. Differences in slope from 1.0 and intercept from 0% were tested for significance using Student's t-test. In addition, Bland-Altman analysis (31), including a calculation of mean bias and the 95th confidence interval, was performed to assess the agreement of MRI and MRS.

Furthermore, the effect of high flip angle imaging was evaluated. For this analysis, relative SNR of magnitude data by imaging flip angle was compared using the nonparametric Friedman test, supplemented by a post hoc analysis. In addition, low SNR-images could result in noisy estimates of R2*. This was also investigated, and R2* values were compared for different imaging flip angles, also using a nonparametric Friedman test.

Statistical significance was assumed at a *P*-value of ≤ 0.05. Statistical analysis was performed using SPSS (version 21, IBM Germany, Ehningen, Germany). Plots were created using Sigma Plot (version 12; Systat-Software, Erkrath, Germany).

RESULTS

MRS yielded a mean FF of 11.8 ± 10.0% with a range of 1.7–42.8%. The corresponding R2* values were a mean of 40.3 ± 5.7 s^{-1} with a range of 27.9–50.1s^{-1}.

Figure 1 presents the results in a patient with liver fat, comparing FF estimates obtained with the four different flip angles and MRS (Fig. 1). The results of linear regression analysis including calculation of slope, intercept, and correlation coefficient R^2 for each imaging flip angle are depicted in Table 1. The results show an excellent correlation with R^2 values of approximately 0.9 when comparing MRS derived PDFF with FF across flip angles, and with and without T1 correction. However, overestimation of the FF was observed with increasing flip angles (≥10°) without correction for T1 recovery (Fig. 2a). T1 correction eliminated the overestimation of FF at high flip angles (ie, 10° and 20°). In addition to correcting the slope of the regression, significant differences were observed in the intercept at higher flip angles, which are successfully corrected by T1 correction (Fig. 2b).

Bland-Altman analysis revealed an increased mean bias as a function of the flip angle when no T1 correction was used (flip angle 1°: −1.40 ±2.38%; flip angle 3°: 2.16 ±2.84%; flip angle 10°: 5.79 ±4.46%; flip angle 20°: 9.06 ±5.99%) (Fig. 3). Use of T1 correction reduced mean T1 bias for high flip angles, resulting in comparable values over the entire range of flip angles investigated (flip angle 1°: −1.45 ±2.37%; flip angle 3°: 0.33 ±2.47%; flip angle 10°: 1.01 ±2.79%; flip angle 20°: 1.88 ±3.45%) (Fig. 4).

Significance values for the relative SNR are presented in Table 2. The relative SNR in the magnitude data was increased using flip angles of larger than 1°. For flip angles of 3° and 10°, the relative SNR was comparable but significantly higher than for a flip angle of 1°. Of interest, using a flip angle of 20°, the relative SNR decreased significantly compared with flip angles of 3° and 10°. An example comparing diagnostic image quality of in-phase images acquired with the four flip angles is given in Figure 5.

Mean R2* values for flip angles of 1°, 3°, 10°, 20° were 52.3 ±15.0 s^{-1}, 43.1 ±9.5s^{-1}, 44.2 ±12.6 s^{-1}, and 47.8 ±20.3 s^{-1}, respectively. R2* values were significantly lower for flip angle 3° compared to flip angle 1° ($P \leq 0.001$) and flip angle 10° compared with flip angle 1° ($P = 0.003$) (Fig. 1). There was no significant difference between flip angle 1° versus 20° ($P = 0.272$); flip angle 3° versus 10° ($P = 1.000$); flip angle 3° versus 20° ($P = 0.060$); and flip angle 10° versus 20° ($P = 0.763$).

DISCUSSION

In this study, we investigated the T1 bias in chemical shift-encoded FF estimates resulting from high flip angles. The use of high flip angles without correction for T1 resulted in strong overestimation of the FF in comparison to MRS. Overestimation of FF can be eliminated by use of T1 correction (20) using published T1 values of liver (809 ms) and fat (382 ms) for

3T (26). The clinical impact of high flip angle imaging was also investigated. Our results demonstrated no advantage of high flip angle imaging for liver fat quantification as compared to low flip angle imaging. However, the higher SNR performance of the underlying source images might be relevant for diagnostic assessment of the liver. Furthermore, low SNR imaging influences R2* mapping related to increased baseline noise, which may ultimately also lead to inaccurate quantification of liver iron content for fat-corrected R2* mapping techniques (32).

Recent studies demonstrated that T1 bias is a strong confounder for assessment of liver fat (22,23). We confirmed previous results and revealed an accurate agreement in fat quantification between MRS and chemical shift-encoded MRI using low flip angles.

However, our results clearly indicate that a high flip angle improves the SNR performance of the underlying images at the different echo times, which fundamentally influences image quality. In theory, use of the Ernst angle to maximize SNR performance of spoiled gradient echo acquisitions using the T1 values from (19) and the fixed TR of 6.51 ms (used in this study) are 10.6° for fat and 7.3° for liver (water signal). We confirmed this theoretical calculation and revealed a maximum relative SNR or, respectively, highest quantitative image quality using flip angle of 10° followed by 3°. When imaging above the Ernst angle (eg, 20°) there is no benefit because these acquisitions result in a high T1 related bias and reduced SNR performance compared with images acquired at or near the Ernst angle.

High SNR images are also important for accurate R2* mapping. When chemical shift encoded fat-corrected R2* mapping is used, accurate quantification of liver iron overload is possible, even in the presence of fat (25,32–34). Low SNR images with increased noise may reduce the accuracy of R2* mapping. Therefore, data acquisition at the Ernst angle may be important for iron quantification. Further investigation of this observation is necessary, particularly in subjects with iron overload.

T1 correction compensates for T1-based errors, yielding reliable and comparable results across flip angles. In our study, we used an offline tool for T1 correction based on published values for tissue fat and liver (26). The T1 values published in this study show a relatively high standard deviation (26). We, therefore, assume that there are possible inter-individual differences in T1 that might affect the accuracy of T1 correction, especially in individuals with chronic liver disease and iron overload (35–37). Individual T1 times could be determined using T1 mapping methods (38). Therefore, in the future, we might be able to assess liver fat on high SNR images without T1 bias using a combination of a T1 corrected chemical shift-encoded MRI and T1 mapping.

Note that very high flip angles may also adversely affect assessment of liver fat; for example very high flip angles are more sensitive to B1 inhomogeneity effects, especially at high field strengths where dielectric effects are important (39,40). Despite this concern, this effect was not observed in our study performed at 3T, where excellent agreement between MRS and T1-corrected high flip angle MRI was demonstrated. However, the correlation between both techniques slightly decreases as a function of the flip angle. Additionally, the intercept of the comparison between MRS and chemical shift imaging increases as a function of the flip

angle, especially in FF without T1 correction and might impair liver fat quantification. These observations warrant further investigation.

Our study has several limitations. First, the size of the study population is small and other chronic liver diseases were not considered. This may be relevant in individuals with chronic liver diseases such as liver iron overload (35), fibrosis (36), and cirrhosis (37) where the T1 may vary in these pathologies. Second, we used MRS as standard of reference. Although MRS is an accurate technique for assessment of liver fat, it is prone to sampling errors. Therefore, our statistical analysis may be affected by sampling errors. Another limitation of this study is the use of a three-echo technique with unequal echo spacing (out-of-phase, in-phase, in-phase). However, at this time, it is not clear how many and which echoes are required for an accurate assessment of liver fat. Similar to recent studies (15,41) our results reveal excellent agreement between MRI and MRS if the measurement is either T1-independent (low flip angle) or if T1 correction is used. Furthermore, the imaging data in this study were acquired using parallel imaging to facilitate breathhold imaging. The use of parallel imaging leads to a spatially dependent noise. We avoided this problem by using relative SNR between flip angles (27). This approach assumes that the spatial dependence of noise in the acquisition did not vary between flip angle acquisitions, which is thought to be a reasonable assumption. Finally, our study protocol included only four sequences with flip angles 1°, 3°, 10°, and 20°. For a complete characterization of T1-bias and T1-correction in assessment of liver fat, acquisition of more flip angles with a constant increment in the range 1–20° may be advantageous.

In conclusion, T1 bias is a strong confounder for assessment of liver fat and depends on the amount of fat present and the flip angle used for image acquisition. Using T1-independent measurements with low flip angles, we found an excellent agreement between MRS and MRI. However, very low flip angle imaging results in low SNR magnitude data, which might be relevant for diagnostic liver imaging and leads to inaccurate R2* estimation. For this reason, we recommend the use of a flip angle near the Ernst angle in combination with T1 correction as an alternative to low flip angle imaging, when the echo images and R2* estimates are important for the clinical exam. T1 correction can performed in a postprocessing step using static T1 values for liver tissue and fat obtained at 3T. The combination of high flip angle imaging and T1 correction generates high SNR images and results in an excellent agreement between MRS and MRI in estimating liver fat content.

Acknowledgments

Contract grant sponsor: the German Federal Ministry of Education and Research; Contract grant number: FKZ 03IS2061A; Contract grant sponsor: the Ministry of Cultural Affairs of the Federal State of Mecklenburg-West Pomerania; Contract grant number: UG 09 033; Contract grant sponsor: the Deutsche Krebshilfe/Dr. Mildred-Scheel-Stiftung; Contract grant number: 109102; Contract grant sponsor: Deutsche Forschungsgemeinschaft; Contract grant numbers: DFG GRK840-D2/E3/E4, MA 4115/1–2/3; Contract grant sponsor: the Federal Ministry of Education and Research; Contract grant numbers: BMBF GANI-MED 03IS2061A, BMBF 0314107, 01ZZ9603, 01ZZ0103, 01ZZ0403, 03ZIK012; Contract grant sponsor: the European Union; Contract grant numbers: EU-FP-7: EPC-TM, EU-FP7-REGPOT-2010-1.

We thank Danilo Wegner for his help in this work. This work is part of the research project Greifswald Approach to Individualized Medicine (GANI_MED). The GANI_MED consortium is funded by the German Federal Ministry of Education and Research and the Ministry of Cultural Affairs of the Federal State of Mecklenburg-West Pomerania.

References

1. Reeder SB, Sirlin CB. Quantification of liver fat with magnetic resonance imaging. Magn Reson Imaging Clin N Am. 2010; 18:337–357. ix. [PubMed: 21094444]
2. Springer F, Machann J, Claussen CD, Schick F, Schwenzer NF. Liver fat content determined by magnetic resonance imaging and spectroscopy. World J Gastroenterol. 2010; 16:1560–1566. [PubMed: 20355234]
3. Hu HH, Bornert P, Hernando D, et al. ISMRM workshop on fat-water separation: insights, applications and progress in MRI. Magn Reson Med. 2012; 68:378–388. [PubMed: 22693111]
4. Kuehn J-P, Hernando D, Meffert PJ, et al. Proton-density fat fraction and simultaneous R2* estimation as an MRI tool for assessment of osteoporosis. Eur Radiol. 2013 Epub ahead of print.
5. Wren TAL, Bluml S, Tseng-Ong L, Gilsanz V. Three-point technique of fat quantification of muscle tissue as a marker of disease progression in Duchenne muscular dystrophy: preliminary study. AJR Am J Roentgenol. 2008; 190:W8–W12. [PubMed: 18094282]
6. Li J, Xie Y, Yuan F, Song B, Tang C. Noninvasive quantification of pancreatic fat in healthy male population using chemical shift magnetic resonance imaging: effect of aging on pancreatic fat content. Pancreas. 2011; 40:295–299. [PubMed: 21178651]
7. Schuchmann S, Weigel C, Albrecht L, et al. Non-invasive quantification of hepatic fat fraction by fast 1.0, 1.5 and 3.0T MR imaging. Eur J Radiol. 2007; 62:416–422. [PubMed: 17267159]
8. Cassidy FH, Yokoo T, Aganovic L, et al. Fatty liver disease: MR imaging techniques for the detection and quantification of liver steatosis. Radiographics. 2009; 29:231–260. [PubMed: 19168847]
9. Merkle EM, Nelson RC. Dual gradient-echo in-phase and opposed-phase hepatic MR imaging: a useful tool for evaluating more than fatty infiltration or fatty sparing. Radiographics. 2006; 26:1409–1418. [PubMed: 16973772]
10. Chang JS, Taouli B, Salibi N, Hecht EM, Chin DG, Lee VS. Opposed-phase MRI for fat quantification in fat-water phantoms with 1H MR spectroscopy to resolve ambiguity of fat or water dominance. AJR Am J Roentgenol. 2006; 187:W103–W106. [PubMed: 16794122]
11. Reeder SB, Cruite I, Hamilton G, Sirlin CB. Quantitative assessment of liver fat with magnetic resonance imaging and spectroscopy. J Magn Reson Imaging. 2011; 34 spcone.
12. Hines CDG, Frydrychowicz A, Hamilton G, et al. T independent, T(2) (*) corrected chemical shift based fat-water separation with multi-peak fat spectral modeling is an accurate and precise measure of hepatic steatosis. J Magn Reson Imaging. 2011; 33:873–881. [PubMed: 21448952]
13. Hines CDG, Yu H, Shimakawa A, McKenzie CA, Brittain JH, Reeder SB. T 1independent, T 2* corrected MRI with accurate spectral modeling for quantification of fat: validation in a fat-water-SPIO phantom. J Magn Reson Imaging. 2009; 30:1215–1222. [PubMed: 19856457]
14. Yokoo T, Shiehmorteza M, Hamilton G, et al. Estimation of hepatic proton-density fat fraction by using MR imaging at 3.0 T. Radiology. 2011; 258:749–759. [PubMed: 21212366]
15. Meisamy S, Hines CDG, Hamilton G, et al. Quantification of hepatic steatosis with T1-independent, T2-corrected MR imaging with spectral modeling of fat: blinded comparison with MR spectroscopy. Radiology. 2011; 258:767–775. [PubMed: 21248233]
16. Reeder SB, Hu HH, Sirlin CB. Proton density fat-fraction: a standardized MR-based biomarker of tissue fat concentration. J Magn Reson Imaging. 2012; 36:1011–1014. [PubMed: 22777847]
17. Kang GH, Cruite I, Shiehmorteza M, et al. Reproducibility of MRI-determined proton density fat fraction across two different MR scanner platforms. J Magn Reson Imaging. 2011; 34:928–34. [PubMed: 21769986]
18. Bydder M, Shiehmorteza M, Yokoo T, et al. Assessment of liver fat quantification in the presence of iron. Magn Reson Imaging. 2010; 28:767–776. [PubMed: 20409663]
19. Liu C-Y, McKenzie CA, Yu H, Brittain JH, Reeder SB. Fat quantification with IDEAL gradient echo imaging: correction of bias from T(1) and noise. Magn Reson Med. 2007; 58:354–364. [PubMed: 17654578]
20. Hines, CD.; Yokoo, T.; Bydder, M.; Sirlin, CB.; Reeder, SB. Optimization of flip angle to allow tradeoffs in T1 bias and SNR performance for fat quantification. Proceedings of the 18th Annual Meeting of ISMRM; Stockholm, Sweden. 2010;

21. Bydder M, Yokoo T, Hamilton G, et al. Relaxation effects in the quantification of fat using gradient echo imaging. Magn Reson Imaging. 2008; 26:347–359. [PubMed: 18093781]
22. Johnson BL, Schroeder ME, Wolfson T, et al. Effect of flip angle on the accuracy and repeatability of hepatic proton density fat fraction estimation by complex data-based, T1-independent, T2*-corrected, spectrum-modeled MRI. J Magn Reson Imaging. 2013 Epub ahead of print.
23. Yang IY, Cui Y, Wiens CN, Wade TP, Friesen-Waldner LJ, McKenzie CA. Fat fraction bias correction using T1 estimates and flip angle mapping. J Magn Reson Imaging. 2013 Epub ahead of print.
24. Pineda N, Sharma P, Xu Q, Hu X, Vos M, Martin DR. Measurement of hepatic lipid: high-speed T2-corrected multiecho acquisition at 1H MR spectroscopy–a rapid and accurate technique. Radiology. 2009; 252:568–576. [PubMed: 19546430]
25. Kuehn J-P, Hernando D, Munoz Del Rio A, et al. Effect of multi-peak spectral modeling of fat for liver iron and fat quantification: correlation of biopsy with MR imaging results. Radiology. 2012; 265:133–142. [PubMed: 22923718]
26. de Bazelaire CMJ, Duhamel GD, Rofsky NM, Alsop DC. MR imaging relaxation times of abdominal and pelvic tissues measured in vivo at 3.0 T: preliminary results. Radiology. 2004; 230:652–659. [PubMed: 14990831]
27. Reeder SB, Wintersperger BJ, Dietrich O, et al. Practical approaches to the evaluation of signal-to-noise ratio performance with parallel imaging: application with cardiac imaging and a 32-channel cardiac coil. Magn Reson Med. 2005; 54:748–754. [PubMed: 16088885]
28. Gilbert G. Measurement of signal-to-noise ratios in sum-of-squares MR images. J Magn Reson Imaging. 2007; 26:1678–1679. [PubMed: 18059007]
29. Dietrich O, Raya JG, Reeder SB, Reiser MF, Schoenberg SO. Measurement of signal-to-noise ratios in MR images: influence of multichannel coils, parallel imaging, and reconstruction filters. J Magn Reson Imaging. 2007; 26:375–385. [PubMed: 17622966]
30. Yu H, McKenzie CA, Shimakawa A, et al. Multiecho reconstruction for simultaneous water-fat decomposition and T2* estimation. J Magn Reson Imaging. 2007; 26:1153–1161. [PubMed: 17896369]
31. Bland JM, Altman DG. Statistical methods for assessing agreement between two methods of clinical measurement. Lancet. 1986; 1:307–310. [PubMed: 2868172]
32. Hernando D, Kramer JH, Reeder SB. Multipeak fat-corrected complex R2* relaxometry: theory, optimization, and clinical validation. Magn Reson Med. 2013 Epub ahead of print.
33. Sirlin CB, Reeder SB. Magnetic resonance imaging quantification of liver iron. Magn Reson Imaging Clin N Am. 2010; 18:359–381. ix. [PubMed: 21094445]
34. Hernando D, Kuehn J-P, Mensel B, et al. R2* estimation using “in-phase” echoes in the presence of fat: the effects of complex spectrum of fat. J Magn Reson Imaging. 2013; 37:717–726. [PubMed: 23055408]
35. Henninger B, Kremser C, Rauch S, et al. Evaluation of MR imaging with T1 and T2* mapping for the determination of hepatic iron overload. Eur Radiol. 2012; 22:2478–2486. [PubMed: 22645044]
36. Chow AM, Gao DS, Fan SJ, Qiao Z, Lee FY, Yang J, et al. Measurement of liver T1 and T2 relaxation times in an experimental mouse model of liver fibrosis. J Magn Reson Imaging. 2012; 36:152–158. [PubMed: 22334510]
37. Heye T, Yang S-R, Bock M, et al. MR relaxometry of the liver: significant elevation of T1 relaxation time in patients with liver cirrhosis. Eur Radiol. 2012; 22:1224–1232. [PubMed: 22302503]
38. Katsube T, Okada M, Kumano S, et al. Estimation of liver function using T1 mapping on Gd-EOB-DTPA-enhanced magnetic resonance imaging. Invest Radiol. 2011; 46:277–283. [PubMed: 21343827]
39. Zelaya FO, Roffmann WU, Crozier S, Teed S, Gross D, Doddrell DM. Direct visualisation of B1 inhomogeneity by flip angle dependency. Magn Reson Imaging. 1997; 15:497–504. [PubMed: 9223051]
40. Truong, T-K.; Chakeres, DW.; Schmalbrock, P. Effects of B0 and B1 inhomogeneity in ultra-high field MRI. Proceedings of the 12th Annual Meeting of ISMRM; Kyoto, Japan. 2004;

41. Yokoo T, Collins JM, Hanna RF, Bydder M, Middleton MS, Sirlin CB. Effects of intravenous gadolinium administration and flip angle on the assessment of liver fat signal fraction with opposed-phase and in-phase imaging. J Magn Reson Imaging. 2008; 28:246–251. [PubMed: 18581393]

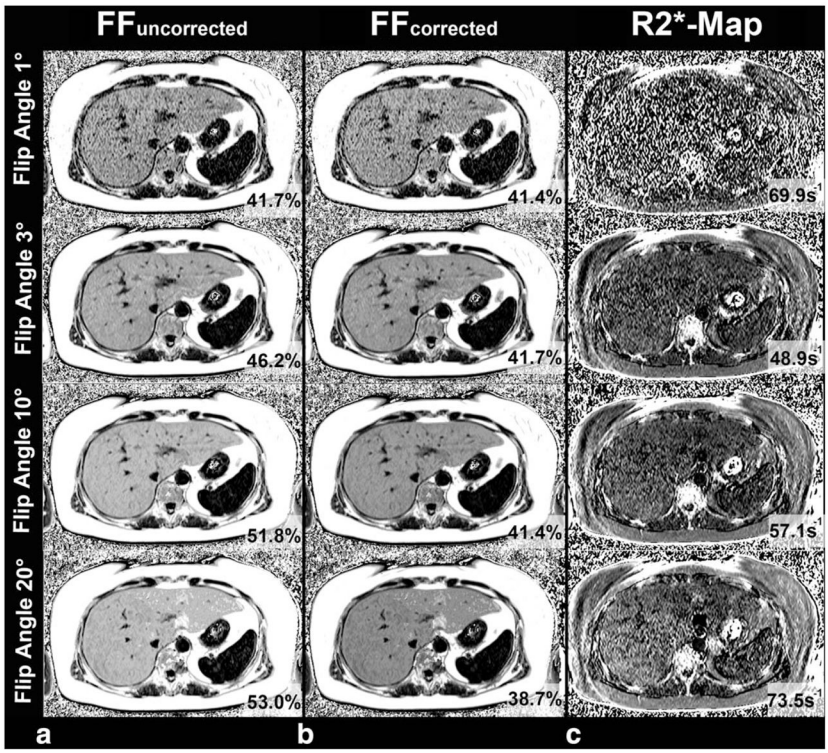

Figure 1.

A 54-year-old patient with fatty liver disease with a fat content of 42.8% demonstrated by MRS. **a:** Without correction of T1 effects, FF estimates increase with the flip angle used for image acquisition. The best agreement was observed for a T1-independent FF using a flip angle of 1°. **b:** Use of correction for T1 bias provides stable results with excellent agreement with between MRI and spectroscopy across all flip angles investigated. **c:** T1-independent imaging using very low flip angles (eg, 1°) and very high flip angles is not recommended because of the lower SNR compared with flip angle 3/10°. This might be clinically relevant for reliable assessment of R2*, which is showing by different R2* values in the same patient measured in the same location.

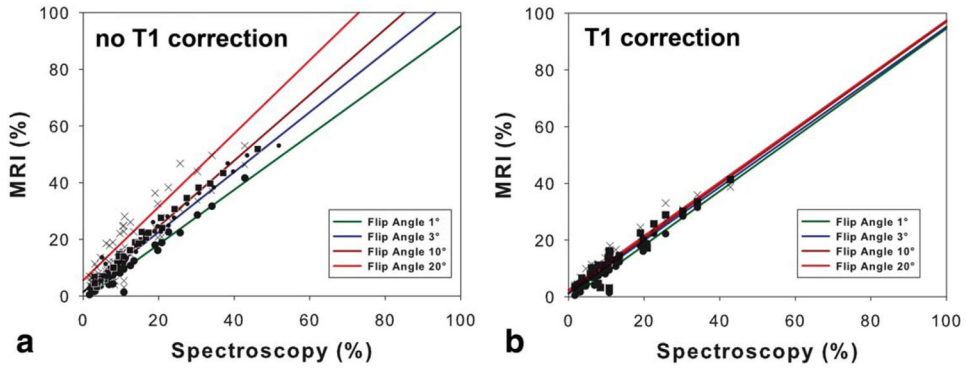

Figure 2.

The graphs show a comparison between fat fractions assessed from chemical shift encoded MRI and MRS. **a:** There is an excellent agreement between MRI and MRS using very low flip angles. Without a correction for T1 recovery there is an overestimation of MRI depending on the flip angle and the liver fat content. **b:** This overestimation is completely eliminated using a T1 correction postprocessing. Consequently, there is an excellent agreement between MRI and MRS over the entire range of flip angles, when using T1-corrected fat quantification.

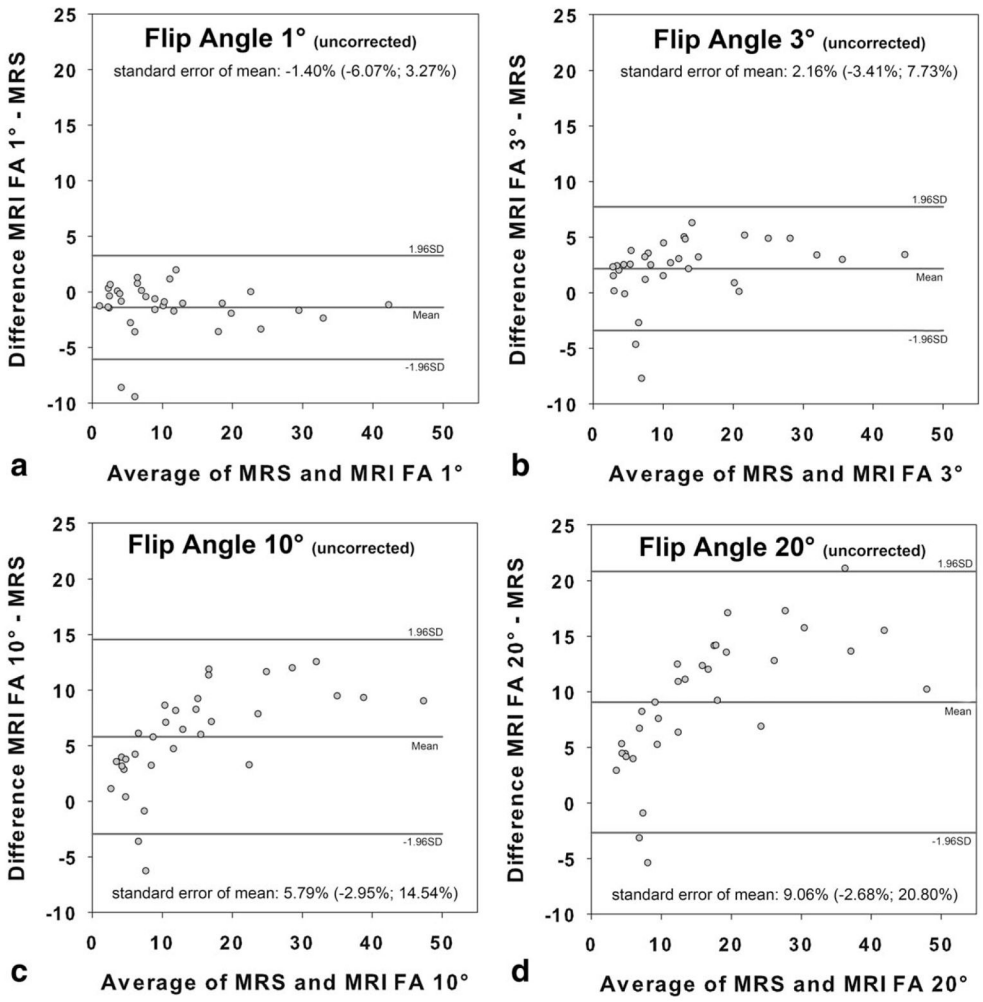

Figure 3.

Fat fractions of MRI in comparison to MR spectroscopy (MRS) for each of the four flip angles *without correction of T1 recovery bias*: 1° (**a**), 3° (**b**), 10° (**c**), 20° (**d**). There is excellent agreement between MRI using flip angles of 1°/3° and MRS. In the presence of fat, errors in fat fraction (FF) estimates increase as a function of the true fat content using higher imaging flip angles of 10°/20°.

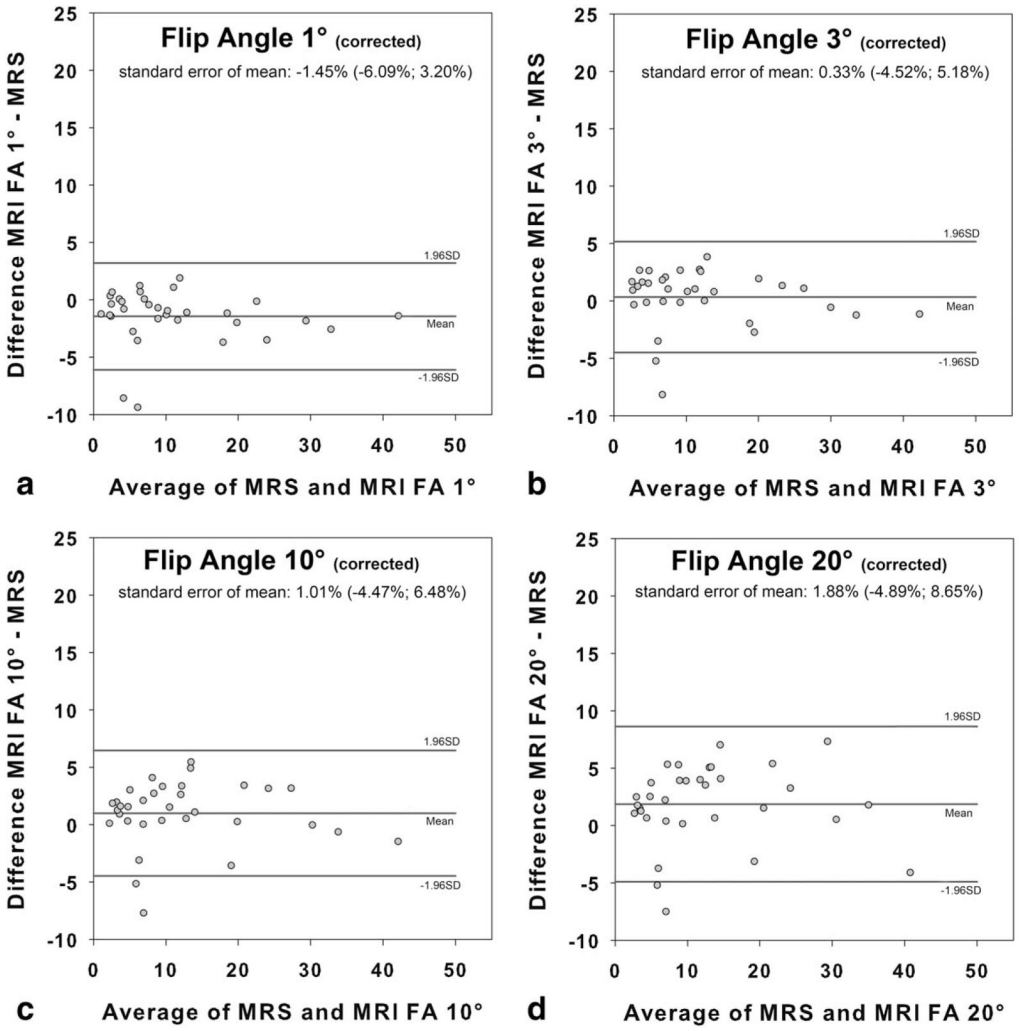

Figure 4.

Fat fractions for each of the four flip angles *with correction of T1 recovery bias*: 1° (**a**), 3° (**b**), 10° (**c**), 20° (**d**). T1 bias correction using assumed T1 values of 382 ms for fat and 842 ms for liver compensates for T1-induced errors in fat fraction over the entire range of flip angles investigated at 3T.

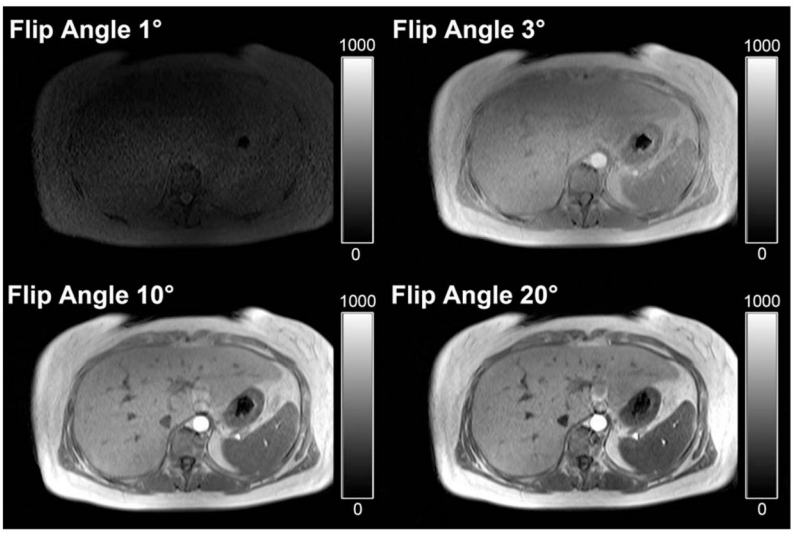

Figure 5.

Magnitude in-phase images of the patient with fatty liver disease presented in Figure 1. **Top Left:** The low SNR caused by very low flip angle imaging negatively influences diagnostic image quality. **Top Right, Bottom Row:** SNR improves significantly with use of higher flip angles for acquisition, resulting in MR images of diagnostic image quality.

Table 1

Correlation Coefficients (R2) and the Slopes/Intercepts Including Corresponding P-Values for the Comparison of Spectroscopy and Fat Fractions Estimated Using Flip Angles of 1°, 3°, 10°, and 20° With and Without T1 Correction*

	Slope	Intercept (%)	R^2
FF-FA 1° Uncorrected	**0.96 (*P*=0.385)**	**−0.94 (*P*=0.187**	0.94
FF-FA 3° Uncorrected	**1.06 (*P*=0.289)**	**1.49 (*P*=0.090)**	0.93
FF-FA 10° Uncorrected	1.21 (*P*=0.016)	3.27(*P*=0.017)	0.91
FF-FA 20° Uncorrected	1.29 (*P*=0.014)	5.58 (*P*=0.005)	0.86
FF-FA 1° T1-corrected	**0.95 (*P*=0.311)**	**−0.91 (*P*=0.194)**	0.94
FF-FA 3° T1-corrected	**0.94 (*P*=0.213)**	**1.02 (*P*=0.163)**	0.94
FF-FA 10° T1-corrected	**0.95 (*P*=0.387)**	**1.54 (*P*=0.077)**	0.92
FF-FA 20° T1-corrected	**0.95 (*P*=0.440)**	2.47 (*P*=0.031)	0.89

* There was excellent agreement of both techniques without T1 correction using low flip angles (ie, 1°/3°) and also for the entire range of flip angles investigated when T1 correction was used. Interestingly, with and without T1 correction, the intercept increased using higher flip angles and might lead to errors in fat quantification.

Table 2

Mean Relative SNR Values and Corresponding Standard Deviations for Magnitude Data (In-Phase Imaging; Out-Phase Imaging) by Flip Angle Used for Data Acquisition*

Mean relative SNR_{IP}		**1°**	**3°**	**10°**	**20°**		**Mean relative SNR_{OP}**
Reference 1	**1°**		$\mathbf{P_{OP} \leq 0.001}$	$\mathbf{P_{OP} \leq 0.001}$	$P_{OP} = 0.420$	**1°**	reference 1
3.2±0.6	**3°**	$\mathbf{P_{IN} \leq 0.001}$		$P_{OP} = 0.272$	$\mathbf{P_{OP} \leq 0.001}$	**3°**	2.9±0.9
3.1±1.1	**10°**	$\mathbf{P_{IN} \leq 0.001}$	$P_{IN} \leq 1.000$		$\mathbf{P_{OP} \leq 0.001}$	**10°**	2.5±1.2
2.2±1.0	**20°**	$\mathbf{P_{IN} = 0.005}$	$\mathbf{P_{IN} \leq 0.001}$	$\mathbf{P_{IN} = 0.001}$		**20°**	1.7±1.0

* The relative SNRs of the magnitude data (in-phase, white background; opposed-phase, gray background) acquired using flip angles of 3° and 10° are higher compared to very low flip angle imaging.